Detecting Food- and Waterborne Viruses by Surface-Enhanced Raman Spectroscopy

Cui Fan, Zhiqiang Hu, Lela K. Riley, Gregory A. Purdy, Azlin Mustapha, and Mengshi Lin

Abstract: Food- and waterborne viruses pose serious health risks to humans and were associated with many outbreaks worldwide. Rapid, accurate, and nondestructive methods for detection of viruses are of great importance to protect public health. In this study, surface-enhanced Raman spectroscopy (SERS) coupled with gold SERS-active substrates was used to detect and discriminate 7 food- and waterborne viruses, including norovirus, adenovirus, parvovirus, rotavirus, coronavirus, paramyxovirus, and herpersvirus. Virus samples were purified and dialyzed in phosphate buffered saline (8 to 9 log PFU/mL) and then further diluted in deionized water for SERS measurement. After capturing the characteristic SERS spectral patterns, multivariate statistical analyses, including soft independent modeling of class analogy (SIMCA) and principal component analysis (PCA), were employed to analyze SERS spectral data for characterization and identification of viruses. The results show that SIMCA was able to differentiate viruses with and without envelope with >95% of classification accuracy, while PCA presented clear spectral data segregations between different virus strains. The virus detection limit by SERS using gold substrates reached a titer of 10^2.

Keywords: gold nanosubstrate, PCA, SERS, SIMCA, virus

Practical Application: SERS is a simple, rapid, and accurate method for detection of food- and waterborne viruses. Our results demonstrate that coupled with gold substrates, SERS was able to rapidly detect and discriminate among different food- and waterborne viruses, indicating that SERS can provide rapid, sensitive, and reproducible detection results with minimum sample preparation for virus detection.

Introduction

Food- and waterborne viruses are important sources causing human diseases. A large number of outbreaks due to viral infections could occur via foods and water contaminated by viruses. Rotavirus, adenovirus, Norwalk-like caliciviruses, and Sapporo-like caliciviruses may cause gastroenteritis in human and animals, which can be diagnosed by a gastroenteritis syndrome, including nausea, water and bloody diarrhea, vomiting, and cramps. Coronavirus and picobirnavirus also may induce a gastroenteritis syndrome. Furthermore, adenoviruses and noroviruses have been proven as the causes for worldwide waterborne disease outbreaks, including the most recently reported adenovirus outbreaks that occurred in Australia in 2000, which led to pharyngoconjunctival fever (Leclerc and others 2002). The adenovirus outbreaks occurred in 5 different countries and 5 different states in the United States in 2009 (Sinclair and others 2009). Additionally, noroviruses are the most common causes of gastroenteritis in United States, which caused multimillion cases of human illness each year. The most recent outbreaks were reported in 2006 in Wisconsin and Florida involving contaminated water in a pool and lake, respectively (Sinclair and others 2009).

MS 20091205 Submitted 12/1/2009, Accepted 2/25/2010. *Authors Fan, Mustapha, and Lin are with Food Science Program, Div. of Food Systems & Bioengineering, author Hu is with Dept. of Civil Engineering, and authors Riley and Purdy are with Dept. of Veterinary Pathobiology, Univ. of Missouri, Columbia, MO 65211, U.S.A. Direct inquiries to author Lin (E-mail: linme@missouri.edu).*

Rapid and accurate detection of viruses is of great importance in controlling and preventing food and waterborne diseases and outbreaks. Common methods for virus detection include electron microscopy (EM) (Stiles and others 2008), cell culture, enzyme-linked immunosorbent assays (ELISA), and polymerase chain reaction (PCR). However, viruses like norovirus cannot grow in a cell culture. EM is used only with a limit of detection around 10^5 to 10^6 particles per milliliter (Koopmans and others 2002). PCR-based molecular methods are still relatively laborious and require complex sample preparations. Therefore, a rapid, simple, and accurate method for detection of food- and waterborne viruses is greatly needed.

Surface-enhanced Raman spectroscopy (SERS) is a type of Raman spectroscopy (Lin and others 2008). In recent years, SERS has been increasingly used in analytical chemistry, food safety, water safety, biological science, antibioterrorism, and other areas (Kneipp and others 2002a; Haynes and others 2005a; Moskovits 2005). Conventional Raman spectroscopy usually generates weak inelastically scattered signals and can only be used for measuring concentrated samples. In the 1970s, scientists discovered the SERS phenomenon in which pyridine molecules were absorbed onto the roughened metallic surface, resulting in a significant enhancement of the Raman signals by many orders of magnitude (Fleischmann and others 1974). Enhanced Raman signals were generated in highly localized optical fields of those metallic structures due to "electromagnetic field enhancement" (Jeanmaire and van Duyne 1977) and "chemical enhancement" of signals (Albrecht and Creighton 1977). Over the last 10 y, with rapid development of nanotechnology and nanomaterials, the interest

doi: 10.1111/j.1750-3841.2010.01619.x

THE Society for Food Science & Technology
Journal of Food Science
A Publication of the Institute of Food Technologists

in SERS was revived. Gold (Au) and silver (Ag) are 2 most commonly used materials for making SERS-active substrates. Other transition metals, such as copper (Cu), rhodium (Rh), and platinum (Pt), could also generate surface enhancement with enhancement factor around 10^4 (Ren and others 2007). SERS could provide "fingerprint-like" spectral information on various chemical and biochemical samples with the limit of detection down to the parts-per-billion (ppb) level or even a single bacterial cell or spore (Kneipp and others 2002a, 2002b; Haynes and others 2005b; He and others 2008a). SERS combined with various substrates has been used to detect respiratory virus and other virus samples with good sensitivity and specificity (Shanmukh and others 2006, 2008; Demirel and others 2009).

The objectives of this study were to investigate the feasibility of using SERS coupled with gold substrates to detect food- and waterborne viruses, including norovirus, adenovirus, parvovirus, rotavirus, coronavirus, the sendai virus, and herpersvirus, and to differentiate the viruses using multivariate statistical analyses (that is, soft independent modeling of class analogy [SIMCA] and principal component analysis [PCA]).

Materials and Methods

Preparation of virus samples

Virus strains were obtained from the Univ. of Missouri Research Animal Diagnostic Laboratory, Columbia, Mo., U.S.A. They included norovirus strain MNV-4 (MNV4), adenovirus strain Mad-1 (MAD), parvovirus strain MVMp (MVM), the simian rotavirus strain SA-11 (SA11), coronavirus strain MHV-A59 (MHV), the sendai virus strain cantell (Sendai), and herpersvirus strain Smith MSGV (MCMV). Virus purification was conducted at 4 °C through a sucrose cushion. The virus precipitate was spun down at 36000 rpm in a swinging bucket rotor (Beckman SW41, Beckman Coulter, Inc., Brea, Calif., U.S.A.) for 3 h before being collected. The interphase on the top layer containing purified viruses was collected and dialyzed in phosphate buffered saline (PBS, pH 7.4; 0.2 g of KH_2PO_4, 1.5 g of $Na_2HPO_4 \cdot 7H_2O$, 8.0 g of NaCl, and 0.2 g of KCl in 1 L of distilled water). The concentrations of the purified virus samples were 8 to 9 log plaque forming units (PFU)/mL. These samples were further diluted 100 times in deionized water before use.

Because virus samples were stored in PBS, we examined whether PBS itself confounded SERS signals of the viruses by comparing the SERS spectra of virus samples in PBS with the spectra of viruses in water. Two virus samples were used for comparison: MAD and SA11. Briefly, an aliquot of MAD (or SA11) in PBS and an aliquot of MAD (or SA11) in water were applied onto a substrate for SERS spectral acquisition. Purified virus samples were prepared in deionized water via a washing step from virus samples stored in PBS.

SERS-active substrates

Klarite™ (D3 Technologies Ltd., Glasgow, U.K.) SERS-active substrates were used in this study. These devices were fabricated on silicon wafers coated with gold. A 6 × 10 mm chip including a 4 × 4 mm patterned SERS-active area and an unpatterned gold reference area was adhered to a standard glass slide. Prepared samples were transferred from 1.5 mL eppendorf tubes using 10 μL pipetman. The samples were deposited onto the substrate for Raman measurement after drying.

Instrumentation

A Renishaw RM1000 Raman spectrometer system (Gloucestershire, U.K.) equipped with a Leica DMLB microscope (Wetzlar, Germany) was used in this study. This system is equipped with a 785 nm near-infrared diode laser source. During the measurement, light from the high power (maximum at 300 mW) diode laser was directed and focused onto the sample at a microscope stage through a 50× objective. Raman scattering signals were detected by a 578 × 385 pixels CCD array detector. The size of each pixel was 22 × 22 μm. Spectral data were collected by WiRE 1.3 software (Gloucestershire, U.K.). Spectra of each virus sample were collected using a 50× objective with a detection range from 300 to 2200 cm^{-1} in the extended mode. The measurement was conducted with a 10 s exposure time and approximately 30 mW laser power (He and others 2008b).

Statistical analysis

Data analysis was conducted using Delight software (D-Squared Development Inc., LaGrande, Oreg., U.S.A.). Pre-processing algorithms were employed to analyze the data, such as smoothing, and 2nd-derivative transformation. Smoothing eliminates high-frequency instrumental noises by averaging neighboring data points. Second-derivative transformation separates overlapping bands and removes baseline offsets. Two multivariate analyses (that is, SIMCA and PCA) were used to analyze spectral data. PCA reduces a multidimensional data set to its most dominant features, removes random variation (noise), and retains the principal components (PCs) that capture the variation between samples treatments (Al-Holy and others 2006; He and others 2008a). SIMCA was used to classify each class of microorganisms according to its analogy to the training samples. SIMCA is based upon a PCA model generated for each class in the training set and assign samples into 2 groups according to their analogy to the class models (Al-Holy and others 2006).

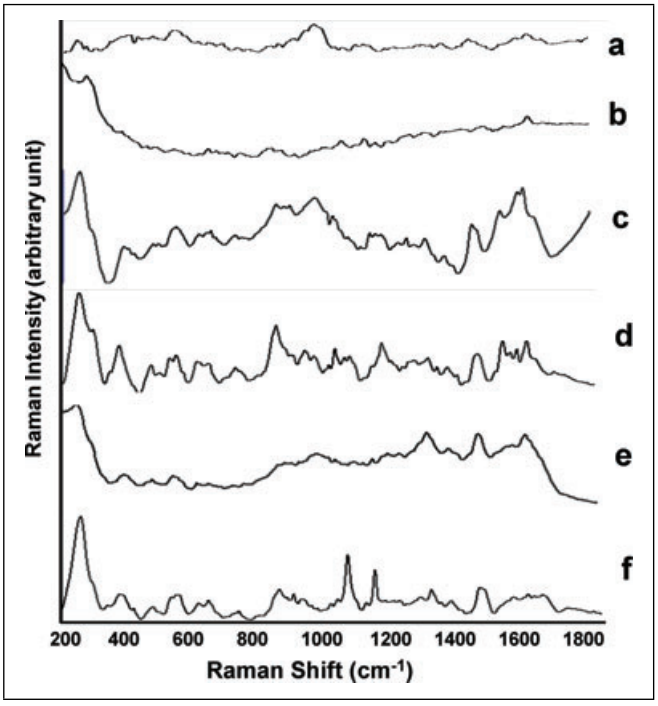

Figure 1–Average SERS spectra (n = 5) acquired from PBS (a), water (b), MAD in PBS (c), MAD in water (d), SA11 in PBS (e), SA11 in water (f). Measurements were conducted from 200 to 1800 cm^{-1} with a 10-s exposure time and approximately 20 mW laser power. Spectra were presented with smoothing at 4 cm^{-1} and baseline adjustment by subtracting a 2nd-order polynomial function.

Results and Discussion

SERS spectra of viruses in different background media

SERS signals acquired from virus samples consist of signals from nucleic acids, proteins, lipids, and carbohydrates (Chu and others 2008). To detect and identify viruses, it is important to differentiate and characterize the specific SERS information of each individual virus. Figure 1 shows the SERS spectra of PBS (Figure 1a), water (Figure 1b), MAD in PBS (Figure 1c), MAD in water (Figure 1d), SA11 in PBS (Figure 1e), and SA11 in water (Figure 1f). There were some clear differences in spectral features of different viruses in PBS and in water. For MAD (Figure 1c and 1d), the peak positions in SERS spectra acquired from the samples containing different background media (PBS or water) were similar. However, the SERS spectra of water background exhibited higher resolution and provided more information on the virus samples. For SA11 (Figure 1e and 1f), 2 intense peaks at around 1100 cm^{-1} were well displayed in the spectrum of water background, but not in the spectrum of PBS background. Therefore, water appeared to be a better background medium for virus detection by SERS as compared with PBS. High-resolution spectra were obtained from the virus samples suspended in water because water contains less interfering compounds compared to PBS. Fewer peaks were observed in Figure 1e than in Figure 1f because the peaks of interfering compounds in PBS overlapped with virus peaks. Thus, it is suggested to include washing and centrifugation steps in the SERS detection procedure. Appropriate dilution in deionized water for virus samples in PBS, a hundred-fold in this study, was set as a standard protocol for all virus sample preparation in the following tests.

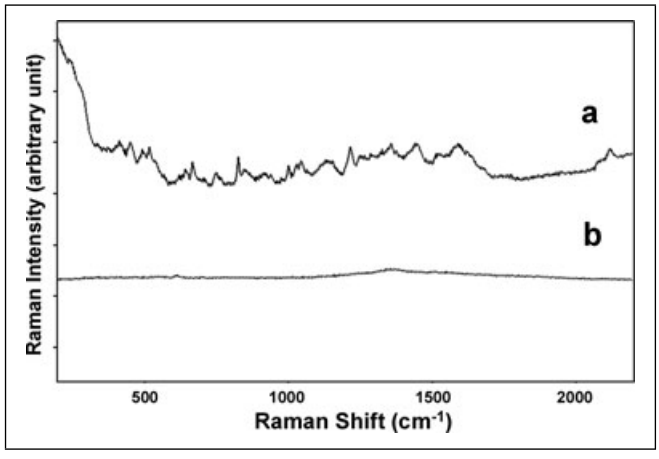

Figure 2–SERS spectrum (a) and conventional Raman spectrum (b) of MNV4.

Conventional Raman compared with SERS

To determine the enhancement performance of Klarite substrates for virus samples, MNV4 samples diluted 100 times by deionized water were deposited onto a Klarite substrate and the control (a gold-coated glass slide without nanostructures), respectively. Figure 2 presents the conventional Raman and SERS spectra of MNV4, demonstrating a significant increase in both Raman peak intensity and spectral resolution by SERS. The results clearly demonstrate that SERS coupled with Klarite can effectively characterize virus samples and provide spectral information with high resolution, and, thus, could serve as a sensitive and nondestructive tool for virus detection. Klarite substrate is one of a few commercial SERS substrates on the market. It has an enhancement factor of 10^4 to 10^5 and its performance is stable and reproducible. Other commercial substrates such as silver colloidal solutions could reach an enhancement factor of 10^7. However, it is difficult to obtain reproducible SERS spectra using colloidal solution substrates in SERS measurement. For these reasons, in this study, Klarite substrate was chosen for virus measurement instead of colloidal solution substrate. Unlike the measurement using colloidal substrates, the use of Klarite requires transferring samples onto substrate surface and drying the sample before SERS measurement. Recently, tip-enhanced Raman spectroscopy (TERS) has been used to directly detect single viruses with a spatial resolution of less than 50 nm (Cialla and others 2009). However, it requires TERS to combine with atomic force microscopy (AFM), which makes the analysis more complex and expensive. Additionally, TERS could hardly differentiate the concentration differences of viruses (Cialla and others 2009).

SERS spectra of infected or uninfected cell lysate and purified viruses

To investigate whether SERS measurement is influenced by biological media or background such as cell lysate, the SERS spectra of uninfected vero cell lysate, MNV4-infected vero cell lysate, and purified MNV4 were obtained and compared (Figure 3). SERS

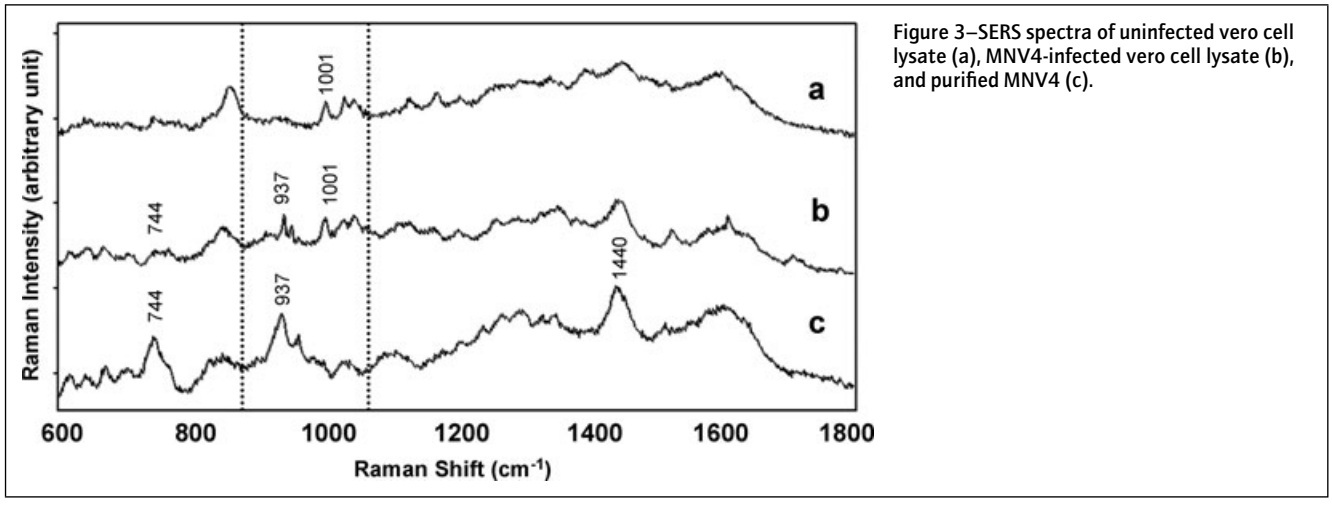

Figure 3–SERS spectra of uninfected vero cell lysate (a), MNV4-infected vero cell lysate (b), and purified MNV4 (c).

spectra collected from multiple different spots on the SERS substrate of the same sample were similar except for minor differences in relative band width and intensity. In the SERS spectrum of uninfected cell lysate (Figure 3a), the bands may be attributed to typical biological components of cells, such as nucleic acids, proteins or amino acids. For example, a band at 1001 cm^{-1} arises from the symmetric ring breathing mode of phenylalanine. For the spectrum of the mixture of cell lysate and viruses (Figure 3b), the bands at 744 and 937 cm^{-1} are linked to viruses, while other bands are from the cell lysate background, such as cell debris. In

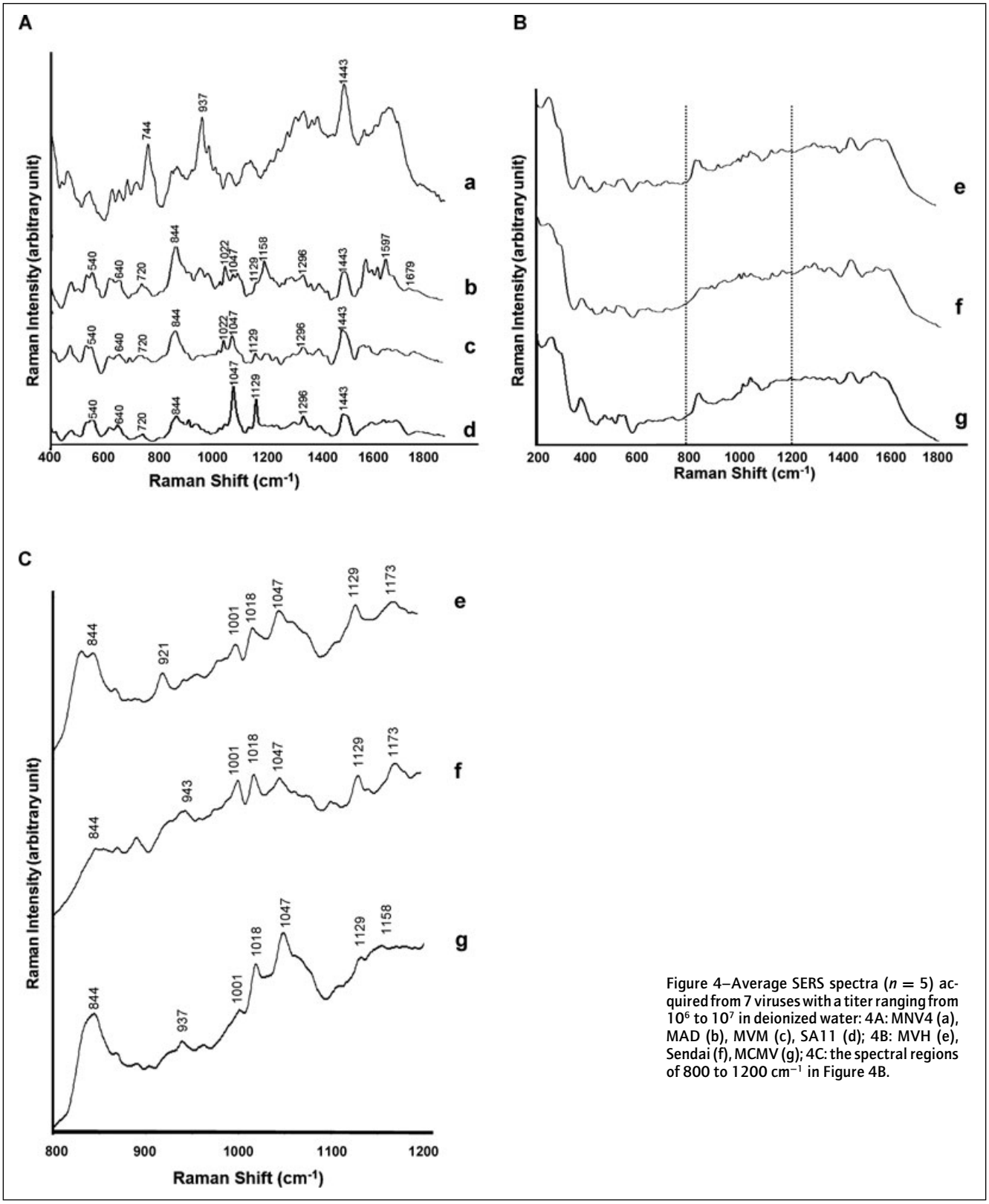

Figure 4–Average SERS spectra ($n = 5$) acquired from 7 viruses with a titer ranging from 10^6 to 10^7 in deionized water: 4A: MNV4 (a), MAD (b), MVM (c), SA11 (d); 4B: MVH (e), Sendai (f), MCMV (g); 4C: the spectral regions of 800 to 1200 cm^{-1} in Figure 4B.

the SERS spectrum of purified MNV4 (Figure 3c), the bands at 744 and 937 cm^{-1} arise from the key features of purified MNV4, which are likely to be adenine and C-COO^- stretch, respectively (Naumann 2001; Schwartzberg and others 2004; Kattumuri and others 2006). These results demonstrate that SERS was able to detect virus from a virus/cell lysate mixture.

SERS spectra of food- and waterborne viruses

Average SERS spectra of 7 virus strains are shown in Figure 4. Every virus sample displays fingerprint-like spectral patterns that are related to their unique structural properties. Table 1 shows typical Raman band assignments in the Raman shift region of 500 to 1800 cm^{-1}.

Distinctive spectral features in the SERS spectrum of MNV4 (Figure 4A a) include strong bands at 744 and 937 cm^{-1}, which are similar to those shown in Figure 3. The SERS spectrum of MAD (Figure 4A b) can be characterized by typical features of nucleic acids, amino acids, and other biological components in viruses. Spectral features of biological components were found in the peaks at 640 cm^{-1} (tyrosine) and 720 cm^{-1} (adenine) (Naumann 2001; Schwartzberg and others 2004; Kattumuri and others 2006). Spectral features of amino acids were found in the peaks at 844 cm^{-1} (tyrosine), 1022 cm^{-1} (the in-plane C–H bending mode of phenylalanine), and 1597 cm^{-1} (tyrosine) (Naumann 2001; Podstawka and others 2004; Schwartzberg and others 2004). The peaks at 540, 1296 cm^{-1} can be attributed to S–S stretch, CH_2 deformation; while peaks at 1047, 1129, and 1159 cm^{-1} was assigned to C–N and C–C stretch (Naumann 2001). The main features of the SERS spectrum of MAD are the strong bands at 844 cm^{-1} (tyrosine) and 1158 cm^{-1} (C–C stretch). These results are in accord with a previous study about adenovirus (Naumann 2001) in which strong bands of nucleic acids were found in MAD. In addition, the band at 1158 cm^{-1} (C–C stretch) is also strong in MAD spectra. The SERS spectrum of MVM (Figure 4A c) has several characteristic bands at 844 (tyrosine), 1022 (phenylalanine), 1047 (C-N stretch), and 1443 cm^{-1} (–CH_2 deformation). In the SERS spectrum of SA-11 (Figure 4A d), the most characteristic bands are at 1047 (C–N stretch) and 1129 cm^{-1} (C–N and C–C stretch). These results demonstrate that subtle compositional differences in nonenveloped viruses could be detected by SERS coupled with gold substrates.

In Figure 4B, 3 typical spectra of enveloped viruses were listed. Compared with the SERS spectra of nonenveloped viruses (4A a–d), the intensities of major peaks are relatively low. However, the SERS spectral features of 3 samples in the regions between 800 and 1200 cm^{-1} clearly differ from each other, which are shown in detail in Figure 4C. For example, in the SERS spectrum of MVH (Figure 4C e), the bands at 844 cm^{-1} (tyrosine) and 921 cm^{-1} (C-COO^- stretch) are distinctive. Interestingly, the C–COO^- stretch bond shifted from the typical 937 to 921 cm^{-1} in different samples probably due to different absorption behavior of samples on the gold substrate. In the SERS spectrum of Sendai (Figure 4C f), the band at 844 cm^{-1} exhibits a relatively lower intensity compared to the bands in the spectra of MVH (Figure 4C e) and MCMV (Figure 4C g); the bands at 1001 cm^{-1} (the symmetric ring breathing mode of phenylalanine) and 1018 cm^{-1} (the in-plane C-H bending mode of phenylalanine) are significant. In the SERS spectrum of MCMV (Figure 4C g), strong peaks are found at 844 (tyrosine), 1018 (phenylalanine), and 1047 cm^{-1} (C–N stretch) compared to the bands in the SERS spectrum of MVH (Figure 4C e) and Sendai (Figure 4C f). These results indicate that even subtle compositional differences in enveloped viruses could be detected by SERS.

Differentiation of enveloped and nonenveloped viruses

Viruses are composed of nucleic acids and a protein coat called capsid. Many viruses, called enveloped viruses, have bilayer lipid envelopes outside the protein capsids. On the contrary, viruses without envelopes are called nonenveloped viruses (Figure 5). Viral envelope is one of the most important parameters to differentiate and classify viruses. For example, enveloped viruses are common among animal viruses while most food-associated viruses are nonenveloped. Therefore, it is important to develop a simple and accurate technique to differentiate between enveloped and nonenveloped viruses. Based on whether or not viruses have an envelope, viruses in this study are classified into 2 groups: MHV, Sendai, and MCMV are enveloped viruses; while MNV4, SA11, MAD, and MVM are nonenveloped viruses. To differentiate between enveloped and nonenveloped viruses, SIMCA was used to analyze spectral data. Figure 6 shows SIMCA classification results of enveloped and nonenveloped viruses. The results show that 41 out of 43 spectra (>95%) of all viruses were correctly

Table 1–Band assignments in the Raman shift region of 500 to 1800 cm^{-1}.[a]

Raman shift (cm^{-1})	Assignment
~ 540	S–S stretch
~ 640	Tyrosine (skeletal)
~ 720, 744	Adenine
~ 844	Tyrosine
~ 921, 937, 943	C–COO^- stretch
~ 1001	Phenylalanine (the symmetric ring breathing mode)
~ 1018, 1022	Phenylalanine (the in-plane C–H bending mode)
~ 1047	C–N stretch
~ 1129	C–N and C–C stretch
~ 1158	C–C stretch
~ 1296	–CH_2 deformation
~ 1325	Adenine
~ 1443	–CH_2 deformation
~ 1597	Tyrosine
~ 1679	Amide I

[a]Adapted from Otto and others (1986), Naumann (2001), Podstawka and others (2004), Schwartzberg and others (2004), and Kattumuri and others (2006).

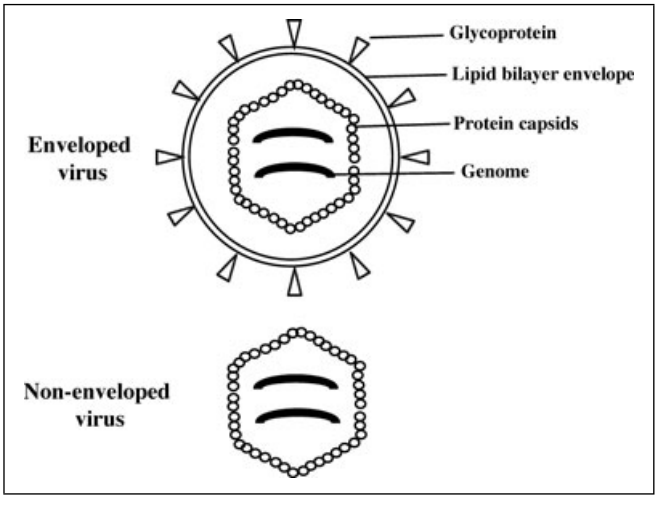

Figure 5–Graphic structures of a typical enveloped virus and a nonenveloped virus.

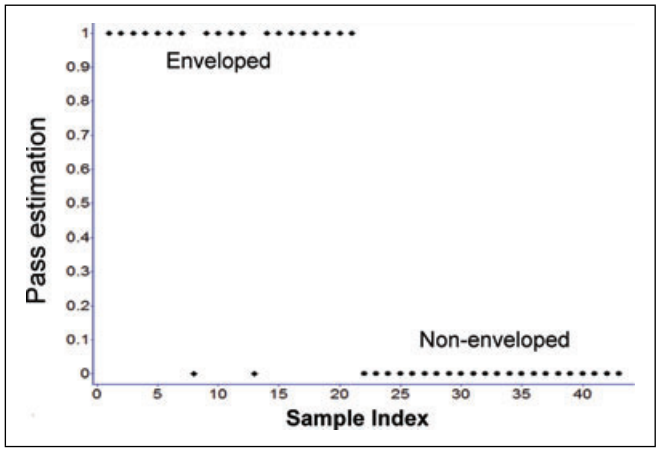

Figure 6–SIMCA classification of enveloped viruses (diamond) and nonenveloped viruses (circle).

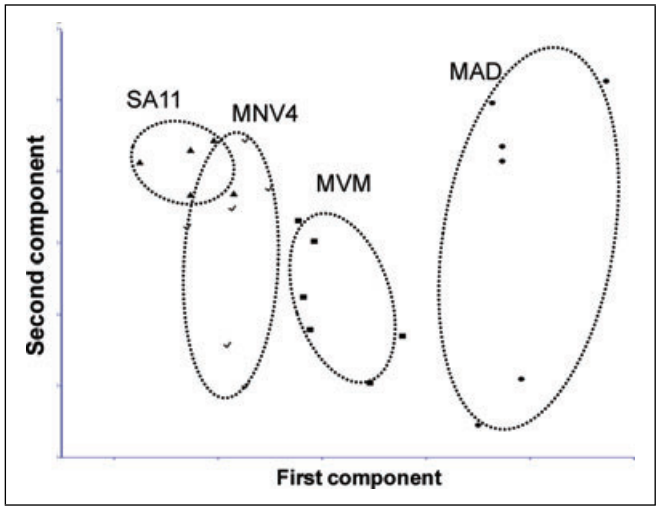

Figure 7–PCA plot based on the SERS spectra acquired from 4 strains of nonenveloped viruses: MAD, MNV4, SA11, and MVM. The PCA model was constructed using the spectral range from 200 to 1800 cm^{-1}.

classified, demonstrating that SIMCA could be used to differentiate enveloped and nonenveloped viruses.

Differentiation of viruses at the strain level

To further investigate the feasibility of using SERS to differentiate different virus species, PCA was conducted based on SERS spectra acquired from 4 nonenveloped virus samples (MNV4, SA11, MAD, and MVM). Clear segregations between most samples were observed although sample clusters of SA11 and MNV4 were partially overlapped (Figure 7). These results indicate that SERS has the potential to differentiate viruses at the strain level. Similar results were obtained for enveloped virus samples. The quantity and distribution of capsid proteins and nucleic acids vary among different viral strains, which could be detected by SERS and revealed in SERS spectral patterns by PCA.

Conclusions

SERS is a simple, rapid, and accurate method for detection of food- and waterborne viruses. Our results demonstrate that it is necessary to dilute virus/PBS samples appropriately in deionized water prior to SERS measurement to minimize the interferences from the PBS buffer. Coupled with Klarite gold substrates, SERS was able to rapidly detect and discriminate among different food- and waterborne viruses. Approximately 95% of virus samples with and without envelop were correctly classified by SIMCA, while PCA could classify and identify different virus samples at the strain level. These results indicate that SERS has a potential for rapid detection and identification of viruses in food and water samples.

Acknowledgments

This study was supported by the U.S. EPA Science to Achieve Results (STAR) project 83384001.

References

Albrecht MG, Creighton JA. 1977. Anomalously intense Raman spectra of pyridine at a silver electrode. J Am Chem Soc 99(15):5215–7.
Al-Holy MA, Lin M, Cavinato AG, Rasco BA. 2006. The use of Fourier transform infrared spectroscopy to differentiate *Escherichia coli* O157:H7 from other bacteria inoculated into apple juice. Food Microbiol 23(2):162–8.
Chu H, Huang Y, Zhao Y. 2008. Silver nanorod arrays as a surface-enhanced Raman scattering substrate for foodborne pathogenic bacteria detection. Appl Spectrosc 62:922–31.
Cialla D, Deckert-Gaudig T, Budich C, Laue M, Möller R, Naumann D, Deckert V, Popp J. 2009. Raman to the limit: tip-enhanced Raman spectroscopic investigations of a single tobacco mosaic virus. J Raman Spectrosc 40(3):240–3.
Demirel MC, Kao P, Malvadkar N, Wang H, Gong X, Poss M, Allara DL. 2009. Bio-organism sensing via surface enhanced Raman spectroscopy on controlled metal/polymer nanostructured substrates. Biointerphases 4(2):35–41.
Fleischmann M, Hendra PJ, McQuillan AJ. 1974. Raman spectra of pyridine adsorbed at a silver electrode. Chem Phys Lett 26(2):163–6.
Haynes CL, Yonzon CR, Zhang XY, van Duyne RP. 2005a. Surface-enhanced Raman sensors: early history and the development of sensors for quantitative biowarfare agent and glucose detection. J Raman Spectrosc 36(6–7):471–84.
Haynes CL, McFarland AD, van Duyne RP. 2005b. Surface-enhanced Raman spectroscopy. Anal Chem 77(17):338A–46A.
He L, Liu Y, Lin M, Mustapha A, Wang Y. 2008a. Detecting single *Bacillus* spores by surface enhanced Raman spectroscopy. Sens Instrum Food Qual Saf 2(4):247–53.
He L, Kim N-J, Li H, Hu Z, Lin M. 2008b. Use of a fractal-like gold nanostructure in surface enhanced Raman spectroscopy for detection of selected food contaminants. J Agric Food Chem 56(21):9843–7.
Jeanmaire DL, van Duyne RP. 1977. Surface Raman spectroelectrochemistry: Part I. Heterocyclic, aromatic, and aliphatic amines adsorbed on the anodized silver electrode. J Electroanal Chem 84(1):1–20.
Kattumuri V, Chandrasekhar M, Guha S, Raghuraman K, Katti KV, Ghosh K, Patel RJ. 2006. Agarose-stabilized gold nanoparticles for surface-enhanced Raman spectroscopic detection of DNA nucleosides. Appl Phys Lett 88(15):153114.
Kneipp K, Kneipp H, Itzkan I, Dasari RR, Feld MS. 2002a. Surface-enhanced Raman scattering and biophysics. J Phys: Condens Matter 14(18):R597–624.
Kneipp K, Haka AS, Kneipp H, Badizadegan K, Yoshizawa N, Boone C, Shafer-peltier KE, Motz JT, Dasari RR, Feld MS. 2002b. Surface-enhanced Raman spectroscopy in single living cells using gold nanoparticles. Appl Spectrosc 56:150–4.
Koopmans M, von Bonsdorff CH, Vinje J, de Medici D, Monroe S. 2002. Foodborne viruses. FEMS Microbiol Rev 26(2):187–205.
Leclerc H, Schwartzbrod L, Dei-Cas E. 2002. Microbial agents associated with waterborne diseases. Crit Rev Microbiol 28(4):371–409.
Lin M, He L, Awika J, Yang L, Ledoux DR, Li H, Mustapha A. 2008. Detection of melamine in gluten, chicken feed and processed foods using surface enhanced Raman spectroscopy and HPLC. J Food Sci 73(8):T129–34.
Moskovits M. 2005. Surface-enhanced Raman spectroscopy: a brief retrospective. J Raman Spectrosc 36:485–96.
Naumann D. 2001. FT-Infrared and FT-Raman Spectroscopy in biomedical research. Appl Spectrosc Reviews 36(2):239–98.
Otto C, Van Den Tweel TJJ, de Mul FFM, Greve J. 1986. Surface-enhanced Raman spectroscopy of DNA bases. J Raman Spectrosc 17:289–98.
Podstawka E, Ozaki Y, Proniewicz LM. 2004. Part I: Surface-enhanced Raman spectroscopy investigation of amino acids and their homodipeptides adsorbed on colloidal silver. Appl Spectrosc 58:570–80.
Ren B, Liu G-K, Lian X-B, Yang Z-L, Tian Z-Q. 2007. Raman spectroscopy on transition metals. Anal Bioanal Chem 388(1):29–45.
Shanmukh S, Jones L, Driskell J, Zhao Y, Dluhy R, Tripp RA. 2006. Rapid and sensitive detection of respiratory virus molecular signatures using a silver nanorod array SERS substrate. Nano Lett 6(11):2630–6.
Shanmukh S, Jones L, Zhao YP, Driskell J, Tripp R, Dluhy R. 2008. Identification and classification of respiratory syncytial virus (RSV) strains by surface-enhanced Raman spectroscopy and multivariate statistical techniques. Anal Bioanal Chem 390(6):1551–5.
Schwartzberg AM, Grant CD, Wolcott A, Talley CE, Huser TR, Bogomolni R, Zhang JZ. 2004. Unique gold nanoparticle aggregates as a highly active surface-enhanced Raman scattering substrate. J Phys Chem B 108(50):19191–7.
Sinclair RG, Jones EL, Gerba CP. 2009. Viruses in recreational water-borne disease outbreaks: a review. J Appl Microbiol 107(12):1769–80.
Stiles PL, Dieringer JA, Shah NC, van Duyne RP. 2008. Surface-enhanced Raman spectroscopy. Ann Rev Anal Chem 1:601–26.